Chemical Physics 362 (2009) 19–26

Contents lists available at ScienceDirect

Chemical Physics

journal homepage: www.elsevier.com/locate/chemphys

# Time and frequency resolved spontaneous emission from supramolecular pheophorbide-*a* complexes: A mixed quantum classical computation

Hui Zhu, Beate Röder, Volkhard May *

*Institut für Physik, Humboldt-Universität zu Berlin, Newtonstraße 15, D-12489 Berlin, Federal Republic of Germany*

ARTICLE INFO

*Article history:*
Received 16 January 2009
Accepted 30 May 2009
Available online 6 June 2009

*Keywords:*
Time and frequency resolved emission
Electronic excitation energy transfer
Chromophore complexes
Mixed quantum classical methodology
MD simulations

ABSTRACT

A mixed quantum classical methodology is utilized to compute the time and frequency resolved emission spectrum of a chromophore complex dissolved in ethanol. The single complex is formed by a butanediamine dendrimer to which pheophorbide-*a* molecules are covalently linked. The electronic excitations are described in a Frenkel-exciton model treated quantum mechanically and all nuclear coordinates are described classically by carrying out room-temperature MD simulations. Starting with the full quantum formula for the emission spectrum, it is translated to the mixed quantum classical case and used to compute time resolved spectra up to 2 ns. To account for radiative decay the chromophore complex excited-state dynamics have to be described in a density matrix theory. While the full emission spectrum only reflects excited-state decay the introduction of partial spectra allows to uncover details of excitation energy redistribution among the chromophores.



## 1. Introduction

The detection of time and frequency resolved spontaneous emission represents a standard approach to uncover details of excitation energy transfer (EET) in supramolecular chromophore complexes (CC, see, for example, [1–8]). The measured emission rates may offer access to a spatial and energetic redistribution of the photoinduced excitation energy. Pheophorbide-*a* (Pheo) CC studied in [5,6] will be of particular interest for the following. We focus here on those CC build up by butanediamine dendrimers to which Pheo molecules are covalently linked [5] (see also our earlier work in Refs. [9–11]). Different generations of dendrimer Pheo complexes have been synthesized, extending from $P_2$ with two Pheo moieties, over $P_4$ with four (see Fig. 1) up to $P_{32}$ with 32 [5]. After photo excitation the $P_n$ are capable to form Frenkel-exciton states and to generate singlet oxygen. Since the $P_n$ posses a rather flexible structure they may realize conformations where some Pheo molecules are attached close together to form dimers, trimers etc. As already discussed in [9–11] only mixed quantum classical schemes may be ready to simulate the EET which proceeds on the highly flexible structure of the CC. Such a treatment of large molecular systems has been widely described in literature (see the overview in [12] and also [13,14], where a comparison with a complete quantum description of the considered system could be given). It is the task of the present paper to present a mixed quantum classical computation scheme to get time and frequency resolved spontaneous emission spectra. Some preliminary data for $P_4$ in ethanol will be also given.

Full quantum computations of spontaneous emission spectra found huge interest in literature (for a recent overview see [15] and references therein as well as the studies by the Mukamel-group [16–18]). However, to the best of our knowledge, a computation in a mixed quantum classical scheme has never been carried out. In such a scheme usually a quantum simulation of all electronic degrees of freedom is carried out while the nuclear degrees of freedom are put into a classical description [12]. The mixed quantum classical methodology which will be of interest for all subsequent consideration is known as *Ehrenfest dynamics* (see the recent review in [12]). On the one hand it assumes the propagation of the time-dependent electronic wave function depending on the actual nuclear configuration. On the other hand the latter changes according to Newton's equation but in the mean field induced by the actual electronic state. Therefore, the approach accounts for a back reaction of the electron dynamics on that of the nuclei. For the presence of a single excitation in the huge $P_4$ solvent system this back reaction should be of minor importance. Consequently, our MD simulations will be performed in the presence of the CC electronic ground-state force field (according to the size of our system this back reaction would be indeed a challenge for the numerics). We simply arrive at a time-dependent exciton Hamiltonian. Its ingredients, the single chromophore excitation energies $E_m$ and the inter-chromophore Coulomb couplings $J_{mn}$ responsible for excitation energy transfer are considered as time-dependent quantities.

Details of such an approach and the way to compute linear absorbance spectra can be found in [9–11]. Since the inclusion of

* Corresponding author.
*E-mail address:* may@physik.hu-berlin.de (V. May).

0301-0104/$ - see front matter © 2009 Elsevier B.V. All rights reserved.
doi:10.1016/j.chemphys.2009.05.022

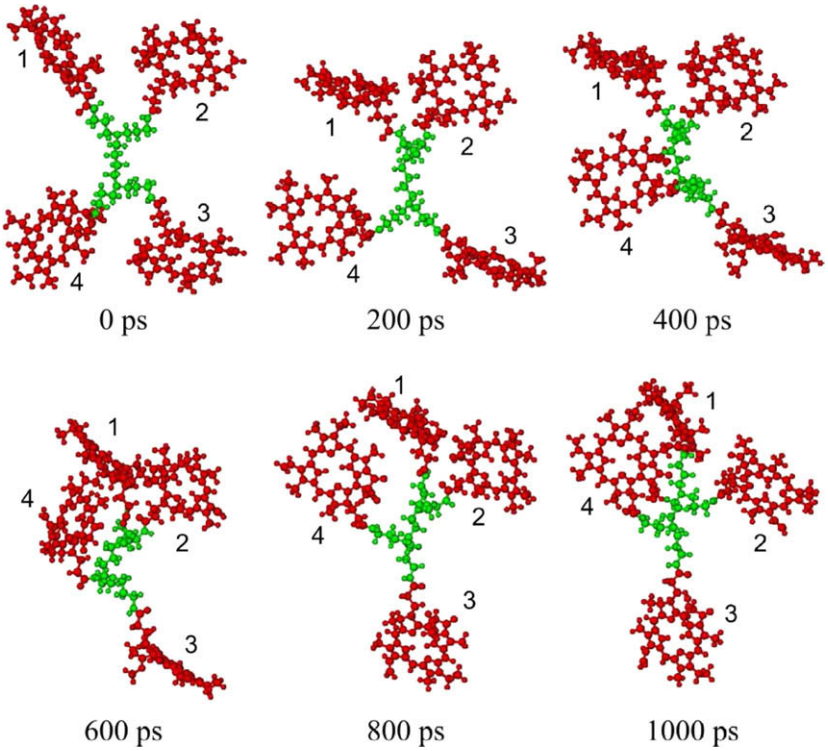


**Fig. 1.** Snapshots of $P_4$ in ethanol along a 1 ns room-temperature MD run (the chromophores have been labeled to identify their changed positions).

permanent charge distributions in the electronic ground- and excited-state of the individual chromophores is indispensable when dealing with Pheo molecules our treatment includes a generalization of the standard Frenkel-exciton theory. Such charge distributions are considered by introducing atomic partial charges. As a consequence, the excited-state modulation of a Pheo molecule caused by its electrostatic coupling to the permanent charge distribution of all other molecules (staying in their electronic ground-state) can be accounted for. Moreover, the excitonic coupling could be calculated nearly exactly by introducing so-called *transition charges* [19]. We also note that the mixed quantum classical description of EET dynamics in CC is valid for any strength of electron (exciton) vibrational coupling. This is in contrast to the full quantum description where it is usually necessary to distinguish between the weak and strong coupling case. And, when extended to a nanosecond time scale (including an ensemble average of those quantities measured in the experiment) the mixed quantum classical description of EET simultaneously accounts for what is often named dynamic as well as static disorder.

The paper is organized as follows. The next section quotes some details of the used Frenkel-exciton model. Section 3 describes the translation of the full quantum formula for the emission spectrum to a mixed quantum classical version (the derivation of the quantum formula is shortly offered in the Appendix A). Preliminary results for $P_4$ in ethanol are presented in Section 4. The paper ends with some concluding remarks in Section 5.

## 2. The model

The used model has been extensively explained recently [10,11]. Here, we shortly review the basic facts of our non-standard Frenkel-exciton description. We first note that within the CC of interest mutual chromophore wave function overlap and electron exchange effects among different chromophores do not take place (absence of the Dexter mechanism). Therefore, we may assume the orthogonality relation $\langle\varphi_{ma}|\varphi_{nb}\rangle = \delta_{m,n}\delta_{a,b}$ to be valid, where $\varphi_{ma}(r_m;R_m)$ denotes the electronic wave function of chromophore $m$ in state $a$ (electronic ground-state: $a = g$, first excited electronic state $a = e$). The electronic coordinates are abbreviated by $r_m$ related to the $m$th chromophore center of mass. (Some of our recent electronic structure calculations for a single Pheo can be found in [20]. They again indicate that for the present purposes only the so-called $Q_y$ state as the first excited singlet state would be of interest. Higher levels are clearly separated.) Moreover, the wave function parametrically depends on all nuclear coordinates $R_m$ of chromophore $m$. The single chromophore electronic Hamiltonian is denoted by $H_m^{(\mathrm{el})}$ and the related potential energy surfaces (PES) by $V_{ma}$. Thus, the approach is based on isolated chromophore quantities with all additional couplings treated separately.

The model used for the total CC is based on an expansion with respect to the CC electronic states. Since wave function overlap between different chromophores can be excluded, the CC ground-state is simply defined as a product of single chromophore electronic ground-state wave functions $\phi_0(r;R) = \prod_m \varphi_{mg}(r_m;R_m)$. Accordingly, the singly excited CC states follow as $\phi_m(r;R) = \varphi_{me}(r_m;R_m)\prod_{n\neq m}\varphi_{ng}(r_n;R_n)$. Double excited CC states are of no interest here. The total Hamiltonian accounts for the CC and its internal coupling (extended later to a coupling to solvent molecules) and a coupling to the radiation field handled classically as well as quantum mechanically:

$$H = H_{\mathrm{CC}} + H_{\mathrm{field}}(t) + H_{\mathrm{CC-phot}} + H_{\mathrm{phot}}. \tag{1}$$

The CC Hamiltonian takes the form

$$H_{\mathrm{CC}} = T_{\mathrm{nuc}} + V_{\mathrm{CC}}, \tag{2}$$

where $T_{\mathrm{nuc}} = \sum_m T_m$ is the kinetic energy operator of all involved nuclear coordinates separated here into the contributions $T_m$ of the various chromophores. The potential $V_{\mathrm{CC}}$ reads in more detail

$$V_{\mathrm{CC}} = \sum_m H_m^{(\mathrm{el})} + \frac{1}{2}\sum_{m,n} V_{mn}. \tag{3}$$

The $V_{mn}$ cover the complete Coulomb interaction between chromophore $m$ and $n$.

An expansion with respect to the CC electronic states gives for the CC Hamiltonian (off-diagonal contributions exist but are of no importance here [11]):

$$H_{\mathrm{CC}} = \mathscr{H}_0|\phi_0\rangle\langle\phi_0| + \sum_{m,n}\mathscr{H}_{mn}|\phi_m\rangle\langle\phi_n| \tag{4}$$

with

$$\mathscr{H}_0 = T_{\mathrm{nuc}} + \mathscr{V}_0(R), \tag{5}$$

and

$$\mathscr{H}_{mn} = T_{\mathrm{nuc}} + \mathscr{V}_{mn}(R). \tag{6}$$

The CC ground-state PES is given by

$$\mathscr{V}_0(R) = \sum_m V_{mg}(R_m) + \frac{1}{2}\sum_{m,n} J_{mn}(gg,gg;R_m,R_n), \tag{7}$$

and that for the singly excited reads

$$\mathscr{V}_{mn}(R) = \delta_{m,n}(\mathscr{V}_0(R) + V_{meg}(R)) + (1-\delta_{m,n})J_{mn}(eg,eg;R_m,R_n). \tag{8}$$

Both CC PES include Coulomb couplings among the electrons and nuclei of all chromophores. The coupling is accounted for by the electronic matrix elements of the overall electrostatic interaction $V_{mn}$ between chromophore $m$ and $n$ [11]. They have the following general structure $(a,b,c,d = g,e)$:

$$J_{mn}(ab,cd) = \int dr_m dr_n \varphi^*_{ma}(r_m)\varphi^*_{nb}(r_n)V_{mn}\varphi_{nc}(r_n)\varphi_{md}(r_m). \tag{9}$$

To carry out the computation of $J_{mn}$ for a particular pair of chromophores we apply the concept of atomic centered partial charges (transition charges) [9,11,19] and write

$$J_{mn}(ab,cd) = \sum_{\mu,\nu}\frac{q_{m\mu}(ad)q_{n\nu}(bc)}{|\mathbf{R}_{m\mu}-\mathbf{R}_{n\nu}|}. \tag{10}$$

The $q_{m\mu}(ad)$ and $q_{n\nu}(bc)$ are charges placed at the atoms of chromophore $m$ positioned at $\mathbf{R}_{m\mu}$ and at the atoms of chromophore $n$ positioned at $\mathbf{R}_{n\nu}$, respectively. If $a = d(b = c)$ the charges represent ordinary ones, but if $a \neq d(b \neq c)$ they are named *transition charges*. As demonstrated in [19], Eq. (10) reproduces exact results nearly perfectly if the charges are properly determined (fit of the electrostatic field). Since this determination is only valid for the electronic ground-state nuclear equilibrium configuration we cannot exclude that their use within MD simulations introduces small errors.

Eq. (7) for $\mathscr{V}_0$ indicates the inclusion of an electrostatic coupling among all chromophores staying in their electronic ground-state. Because of the separate presentation of $\mathscr{V}_0$ in the excited-state PES matrix $\mathscr{V}_{mn}$, Eq. (8), the latter quantity contains ground-state excited-state PES differences, in each case including the Coulomb coupling to all other chromophores:

$$V_{meg}(R) = V_{me}(R_m) + \sum_k J_{mk}(eg,ge;R_m,R_k) - V_{mg}(R_m) - \sum_k J_{mk}(gg,gg;R_m,R_k). \tag{11}$$

This expression shows that an electrostatic coupling between the excited chromophore and all other ones staying in the ground-state is also accounted for.

Solvent solute Coulomb coupling is incorporated by introducing all solvent molecules into the definition of the electronic CC states $\phi_0$ and $\phi_m$ (the excitonic coupling between the solvent and the solute can be ignored and respective polarization contributions are of less importance). Therefore, we multiply the $\phi_0$ and $\phi_m$ by the solvent part $\phi_{\mathrm{sol}} = \prod_{m\in\mathrm{sol}}\tilde{\varphi}_{mg}$ with the single solvent molecule electronic ground-state wave functions $\tilde{\varphi}_{mg}$. As a result, the nuclear kinetic energy operator $T_{\mathrm{nuc}}$ has to include solvent contributions. Moreover, $\mathscr{V}_0$, Eq. (7) may include in its $m$ and $n$ summation solvent contributions. Concerning $\mathscr{V}_{mn}$, Eq. (8), solvent contributions are restricted besides $\mathscr{V}_0$ to the $k$-summations in $V_{meg}$, Eq. (11). Although, polarization forces can be introduced in a similar way we neglect respective contributions and account for them indirectly in using a Pheo excitation energy which has been deduced from the experiment.

We finalize the description of the Hamiltonian, Eq. (1), by focusing on the quantized photon field. It enters via the standard Hamiltonian

$$H_{\mathrm{phot}} = \sum_{\lambda,\mathbf{k}}\hbar\omega_{\mathbf{k}}(a^+_{\lambda\mathbf{k}}a_{\lambda\mathbf{k}} + 1/2), \tag{12}$$

determined by creation and annihilation operators of photons $a^+_{\lambda\mathbf{k}}$ and $a_{\lambda\mathbf{k}}$, respectively (with polarization $\lambda$ and wave vector $\mathbf{k}$). The photon energy is denoted by $\hbar\omega_{\mathbf{k}}$. The coupling of photons to the CC takes the form

$$H_{\mathrm{CC-phot}} = \hbar\sum_{\lambda,\mathbf{k}}\hat{h}_{\lambda\mathbf{k}}(a_{\lambda\mathbf{k}} + a^+_{\lambda\mathbf{k}}), \tag{13}$$

with

$$\hat{h}_{\lambda\mathbf{k}} = \sum_m g_{\lambda\mathbf{k}}(m)|\phi_m\rangle\langle\phi_0| + \mathrm{H.c.}, \tag{14}$$

and with

$$g_{\lambda\mathbf{k}}(m) = -i\sqrt{\frac{2\pi\omega^2_{meg}}{V\hbar\omega_{\mathbf{k}}}}\mathbf{n}_{\lambda\mathbf{k}}\mathbf{d}_m. \tag{15}$$

$V$ denotes the quantization volume, $\hbar\omega_{meg}$ is the basic electronic transition energy in chromophore $m$, and $\mathbf{n}_{\lambda\mathbf{k}}$ the unit vector of transversal polarization. The coupling to the classical radiation field $H_{\mathrm{field}}(t)$ which is responsible for the CC excited-state preparation is of no interest for the following. We introduce the excitation via an appropriate assumption for the EET initial state.

## 3. Mixed quantum classical description of the luminescence spectrum

The standard version of a mixed quantum classical description of molecular dynamics is based on the so-called Ehrenfest dynamics. There, the electronic degrees of freedom are described quantum mechanically using the time-dependent Schrödinger equation

$$i\hbar\frac{\partial}{\partial t}\Phi(r,t;R(t)) = H(R(t);t)\Phi(r,t;R(t)). \tag{16}$$

For the present application, we may take the overall Hamiltonian, Eq. (1) (concerning its dependence on photon contributions we will comment in a moment). The time-dependence of the nuclear coordinates follows from Newton's equation

$$M_\nu\frac{\partial^2}{\partial t^2}\mathbf{R}_\nu(t) = -\nabla_\nu\langle\Phi(t;R(t))|H(R(t);t)|\Phi(t;R(t))\rangle. \tag{17}$$

where $M_\nu$ and $\mathbf{R}_\nu$ are the mass and the coordinate of the $\nu$th nuclei, respectively. The force acting on the nuclei follows from the expectation value of the Hamiltonian taken with the actual electronic wave function.

Since photon contributions enter we have to modify this standard approach by additionally introducing an averaging with respect to photon states. Therefore we replace the expression on the right-hand side of Eq. (17) by $\mathrm{tr}_{\mathrm{phot}}\{\widehat{W}(t)H(R(t);t)\}$, with the trace expression removing photon contributions and with $\widehat{W}(t)$ denoting the overall statistical operator. A similar quantity has been also introduced in the Appendix A, Eqs. (A.1) and (A.5), where

the full quantum formula of the emission rate is given. Here, however, $\widehat{W}(t)$ has to be understood as an operator where the nuclear coordinates enter as classical quantities. But for practical computations this consideration is of minor importance because the *ground-state* classical path approximation is taken, i.e. we use the potential $\langle\phi_0(R(t))|H_{CC}(R(t))|\phi_0(R(t))\rangle$ which, finally, is approximated by a standard MD force field.

Based on this ground-state classical path approximation we presented a detailed discussion of $P_4$ EET dynamics in Ref. [11]. First, such simulations give the probability $P_m(t) = |B_m(t,t_0)|^2$ to have chromophore $m$ in the excited-state. The related probability amplitude $B_m(t,t_0) = \langle\phi_m|\Phi(t,R(t))\rangle$ follows from a projection of the overall wave function into state $\phi_m$. For $P_4$ the probabilities show oscillations in the 0.1 to 1 ps range. This range corresponds to typical values of the excitonic coupling of about 10 meV and less [9]. The $P_m$ as well as $B_m$ are single CC quantities (without any average) which simply follow as the solution of a time-dependent Schrödinger equations with an explicitly time-dependent Hamiltonian. Consequently, the dynamics are completely coherent. Decay of coherence can only be expected when changing from $P_m$ to an ensemble average $\langle P_m\rangle_{ens}$. This has been done in [11] by replacing the ensemble average by a time-averaging $\overline{P}_m$ (with a 10 ps time slice). However, constant chromophore populations as obtained asymptotically in standard density matrix or rate theories does not appear. Instead, all the $\overline{P}_m$ fluctuate around the mean high-temperature population of 1/4 typical for $P_4$. (To relate this type of EET to standard Förster transfer is under progress. We also refer to Ref. [24], where the residues of vibrational overlap in a mixed description of non-adiabatic transitions have been discussed.)

In contrast to our earlier description of EET dynamics in [11], here it is essential to replace the time-dependent Schrödinger equation (16) by an equation for a density operator. This need is already indicated by the full quantum formula for the time and frequency resolved emission (see Appendix A), where EET is accounted for via a reduced density operator from which photon states have been already removed. Moreover, such a reduction becomes also necessary since equations of motion have to be used which include radiative decay. In similarity to Eq. (A.5) we introduce a reduced density operator denoted by $\hat{\sigma}$, which quantum character, however, is only determined by the CC electronic degrees of freedom.

Since exact formulas for time and frequency resolved emission spectra are less standard we shortly present the derivation of the full quantum expressions in the Appendix A (see also [4,15,21]). This full quantum expression, Eq. (A.10), together with the time evolution of the EET density matrix entering Eq. (A.10) have to be translated to a mixed quantum classical version (with all nuclear coordinates handled classically). Unfortunately, there does not exist an unambiguous procedure to get such a mixed quantum classical version (see, for example, [24] and our own discussion in [10,11]). In order to correspond to this uncertainty we first comment on a translation in the absence of excited-state decay. An account for decay processes will be given in the subsequent section.

### 3.1. Translation of the emission rate to the mixed quantum classical case: absence of excited-state decay

If any influence of radiative decay is of less importance (concentration on a time region below 1 ns) one may introduce the density operator entering the emission rate formula, Eq. (A.10), and describing EET according to the following pure state ansatz (at time $\bar{t}$)

$$\hat{\sigma}(\bar{t}) = |\Phi(\bar{t};R(\bar{t}))\rangle\langle\Phi(\bar{t};R(\bar{t}))|. \tag{18}$$

Matrix elements with the excited CC electronic states result in

$$\sigma_{mn}(\bar{t}) = B_m(\bar{t},t_0)B_n^*(\bar{t},t_0), \tag{19}$$

with $B_m(\bar{t}) = \langle\phi_m|\Phi(\bar{t};R(\bar{t}))\rangle$.

Moreover, to translate Eq. (A.10) to the mixed quantum classical case matrix elements of the time evolution operators have to be introduced. The CC ground-state matrix elements of the time evolution operator are replaced, for example, by

$$A_0(t,t_0) = \langle\phi_0|U_{CC}(t,t_0)|\phi_0\rangle, \tag{20}$$

where $U_{CC}(t,t_0)$ is the time evolution operator defined by $H_{CC}(R(t))$ with time-dependent nuclear coordinates (note the initial condition $A_0(t_0,t_0) = 1$). The CC excited-state coefficients describe time evolution starting at the intermediate time $\bar{t}$. They read

$$A_k^*(t,\bar{t};n) = (\langle\phi_k|U_{CC}(t,\bar{t})|\phi_n\rangle)^* = \langle\phi_n|U_{CC}^+(t,\bar{t})|\phi_k\rangle, \tag{21}$$

with $A_k(\bar{t},\bar{t};n) = \delta_{k,n}$. One may combine both coefficients entering Eq. (A.10) to get (note the use of conjugated complex expressions compared with the emission rate formula)

$$\widetilde{A}_k(t,\bar{t};n) = A_0^*(t,t_0)A_0(\bar{t},t_0)A_k(t,\bar{t};n) = A_0^*(t,\bar{t};k)A_k(t,\bar{t};n). \tag{22}$$

Introducing an ordering with respect to the different density matrix elements (see the next section for application) the mixed quantum classical variant of the photon emission rate is written as

$$F(\omega;t) = \sum_{m,n} F_{mn}(\omega;t), \tag{23}$$

with

$$F_{mn}(\omega;t) = \frac{4\omega^3}{3\pi c^3\hbar}\mathrm{Re}\int_{t_0}^{t} d\bar{t}\, e^{-i\omega(t-\bar{t})} \times \langle\sigma_{mn}(\bar{t})\sum_k \widetilde{A}_k^*(t,\bar{t};n) \times [\mathbf{d}_k(t)\mathbf{d}_m^*(\bar{t})]\rangle_{ens}. \tag{24}$$

The various $F_{mn}$ can be considered as partial emission spectra. The bracket $\langle\cdots\rangle_{ens}$ accounts for an averaging with respect to different initial CC solvent nuclear configurations (ensemble average). The time-dependence of the transition dipole moments is understood to be originated by the actual nuclear motion inducing a changing magnitude and spatial orientation according to the formula (remember the introduction of atomic centered transition charges in Eq. (10))

$$\mathbf{d}_m(t) = \sum_{\mu\in m} q_{m\mu}(eg)\mathbf{R}_{m\mu}(t). \tag{25}$$

All introduced coefficients can be calculated by respective equations of motion [9,10] (nonadiabatic couplings have been neglected). We have

$$i\hbar\frac{\partial}{\partial t}A_0(t,t_0) = \mathscr{H}_0(t)A_0(t,t_0). \tag{26}$$

as well as

$$i\hbar\frac{\partial}{\partial t}A_m(t,\bar{t};k) = \sum_n \mathscr{H}_{mn}(t)A_n(t,\bar{t};k). \tag{27}$$

Both equations are combined to

$$i\hbar\frac{\partial}{\partial t}\widetilde{A}_m(t,\bar{t};k) = \sum_n[\mathscr{H}_{mn}(t) - \delta_{mn}\mathscr{H}_0]\widetilde{A}_n(t,\bar{t};k). \tag{28}$$

To compute the emission spectrum according to Eq. (23), first we have to propagate the density matrix $\sigma_{mn}$ up to $\bar{t}$. It describes CC excited-state dynamics initiated by optical excitation (the direct account of this process has been replaced here by a proper choice of the initial density matrix). Next, we need the excited-state matrix element $\widetilde{A}_k^*$ for the time interval between $\bar{t}$ and $t$ (the time-dependent dipole moments are easily calculated). The variation of $\omega$ within this procedure results in the frequency dependency of the spectrum (a possible change from this ideal spectrum to a measured

one is explained in the next section). If the time-dependence of $\sigma_{mn}(\bar{t})$ is slow enough and if the off-diagonal elements are small we arrive at

$$F(\omega;t) \approx \sum_m F_{mm}(\omega;t) = \sum_m \langle \sigma_{mm}(t) \mathscr{I}_m(\omega) \rangle_{\mathrm{ens}}. \quad (29)$$

The emission spectrum is determined by the superposition of (time independent) single chromophore spectra $\mathscr{I}_m(\omega)$ weighted by the actual chromophore population. The thermal averaging (together with the introduction of an additional dephasing factor) reduces the $\bar{t}$ interval on a time region of about $t - 128$ fs. Thus $F(\omega;t)$ follows by an integral starting at $t - 128$ fs up to the actual time $t$.

### 3.2. Translation of the emission rate to the mixed quantum classical case: presence of excited-state decay

When including radiative decay we may again use the translation scheme of the emission rate to a mixed description practiced in the foregoing section. The exception would be, however, the more involved re-interpretation of the density matrix $\hat{\rho}_{mn}$ of the full quantum formula, Eq. (A.10). As discussed previously, it has to be replaced by $\sigma_{mn}$ which is the pendant to $\hat{\rho}_{mn}$ but defined for the case of classically handled nuclear coordinates. Hence, Eq. (A.12) can be adopted but with $\hat{\rho}_{mn}$ replaced by $\sigma_{mn}$ and with the Hamiltonian matrix $\mathscr{H}_{mn}(t)$ now being a time-dependent quantity (due to the time-dependence of the nuclear coordinates). In the same manner we can also use directly Eq. (A.13) as long as radiative decay is concerned (the respective continuum of additional photon states has been removed from the description via introducing a reduced density operator). In the case of non-radiative decay the use of rates is conceptually somewhat questionable (since the vibrational degrees of freedom have been completely considered via MD simulations their indirect account via non-radiative rates would led to a double count, see the discussion in [23]).

## 4. The $P_4$ luminescence spectrum

Nuclear dynamics of the $P_4$ solvent system have been accounted for by carrying out MD simulations of a single CC placed in a box of 1148 ethanol molecules at room-temperature and at normal pressure (simulation of a *NpT*-ensemble). In order to do this the NAMD program package [25] has been used together with the AMBER force field of parm99 and the GAFF parameter sets [26,27] (for further details see [10,11]). The coordinates of all atoms were recorded every 2 fs, and were used to construct the time-dependent CC Hamiltonian including the solvent-induced chromophore excitation energy shifts. So far it was not possible to account for the intra chromophore coordinate dependence of the single chromophore PES $V_{ma}(R_m)(a = g, e)$. But this missing additional source of electronic energy level fluctuation can be compensated by an appropriately chosen overall dephasing time $\tau_{\mathrm{deph}}$ entering $F(\omega;t)$, Eq. (23), as $\exp(-(t-\bar{t})/\tau_{\mathrm{deph}})$ (see also Ref. [10]).

Since the CC exciting external field is outside the scope of the present considerations we have to account for it by establishing appropriate initial conditions. To have some reference data, we, first, assume equal population of all four chromophores (balanced initial excitation). Then, the population is related to the mutual orientation of the transition dipole moment and the electric field vector what is considered as a rather realistic choice for the initial state (unbalanced initial excitation). The absence of inter-chromophore coherences in both cases is justified by the particular way of excitation chosen in the experiment [5], where photon absorption in the $S_2$-state region has been realized within a sub-ps time interval followed by a subsequent sub-ps internal conversion to the $S_1$-state.

### 4.1. Balanced initial excitation energy distribution

For the initially excited-state of $P_4$ we assume here excitation energy localization at the chromophores with equal probability, i.e. $\sigma_{mn}(t_0) = \delta_{m,n}/4$. The ideal time and frequency resolved emission spectrum of $P_4$ (cf. Fig. 1) is depicted in Fig. 2. This frequency resolved emission spectrum (together with the related frequency integrated spectrum) clearly displays radiative decay. To correspond to the experimentally observed decay [5], we took an overall decay rate with $1/k = 3.5$ ns.

The numerical effort to compute the spectrum has restricted the ensemble average to the use of data corresponding to 10 different MD runs. As also done for all following spectra it has been normalized by its maximum. The rather flat data are due to the use of curves displaying the frequency resolved emission every 6 ps. But the performed averaging with respect to 10 MD runs and the use of a dephasing time $\tau_{\mathrm{deph}}$ of 20 fs have also a particular influence (this value came out from our studies in Ref. [10] on the CC absorbance).

A time trace of Fig. 2 taken at the absorption maximum is shown in Fig. 3. To compare the computed emission with measured data the ideal spectrum $F(\omega;t)$, Eqs. (23) and (24) has to

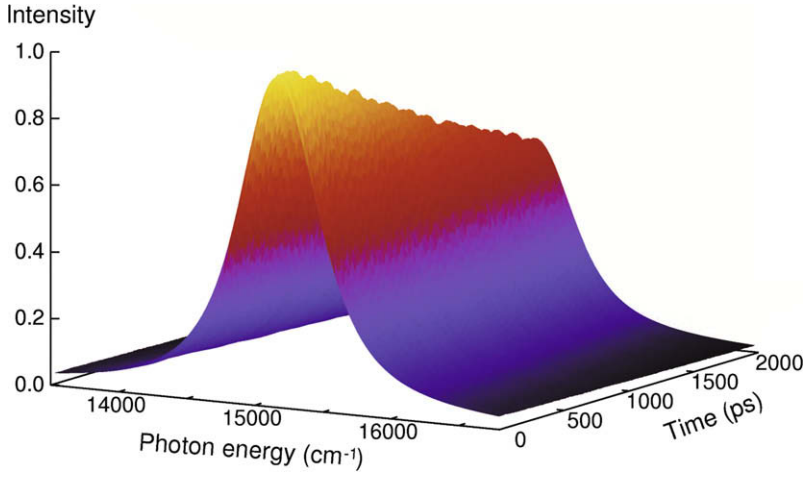


**Fig. 2.** Ideal time and frequency resolved emission spectrum of $P_4$ (normalized by its maximum and averaged by 10 MD runs as well as a dephasing time of 20 fs). The initial excitation corresponds to an equal distribution of population and the absence of inter-chromophore correlations, i.e. $\sigma_{mn} = \delta_{mn}/4$ (for more details see text).

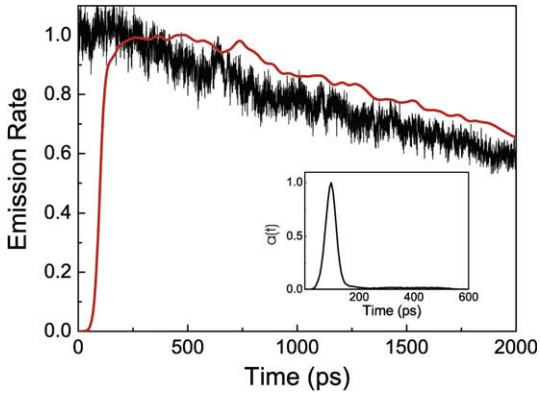


**Fig. 3.** Time resolved emission of $P_4$ as in Fig. 2 but taken at the photon energy of $15,015\ cm^{-1}$ (black line, time step 168 fs). The emission convoluted with an apparatus function (see inset and the text for more details) is shown by the gray line (red online).

be convoluted with an apparatus function $a(t)$ stemming from a single photon counting experiment (see insert of Fig. 3 and [5]):

$$\overline{F}(\omega;t) = \int_0^\infty d\tau a(\tau) F(\omega; t-\tau). \tag{30}$$

The respective curve which follows from this relation is also given in Fig. 3 and matches the measured decay curve of Ref. [5].

In the displayed 2 ns time region we do not find any signature of EET. According to our recent studies of EET in Ref. [11] this had to be expected. There, we observed a redistribution of excited-state population from an initially unbalanced distribution within less than 200 ps. It was followed by a rather chaotic excitation energy oscillation among all four chromophores but roughly with an equal distribution of population at an average. The behavior differs if initially a dimer (two closely arranged chromophores) is prepared (its formation within a single MD run, however, is rather improbable [10,11]).

To get a closer view on the EET dynamics directly after CC excitation the ideal emission spectrum of Fig. 3 has been inspected within a time window of the first 80 ps after preparation of the initial state (not shown). This higher time resolution does not offer any indication of initial excitation energy redistribution. The explanation is also simple. Using the initial condition of equal chromophore population we prepared the equilibrium state of the excited CC (in the mixed quantum classical description). Any change of population is only due to radiative decay (not visible on the 80 ps time scale).

### 4.2. Unbalanced initial excitation energy distribution

To carry out the simulations with a more realistic initial state we populated the different chromophores according to the actual excitation. The direct population of the $S_2$-state of the chromophores gives a value $\sim |\mathbf{d}_m\mathbf{E}|^2$ (to stay simple we used the transition dipole moment into the $S_1$-state, $\mathbf{E}$ is the electric field-strength amplitude). Fast internal conversion results in a respective population of the $S_1$-state and we may set

$$\sigma_{mn}(t_0) = \delta_{m,n} \frac{|\mathbf{d}_m\mathbf{E}|^2}{\sum_k |\mathbf{d}_k\mathbf{E}|^2}. \tag{31}$$

Note, that the non-radiative transitions have destroyed any coherences among different chromophores, but the orientation of the CC with respect to the exciting field has been considered. Of course, in such a case it becomes necessary to carry out a complete orientational averaging. This was not possible. Instead, to have some characteristic non-balanced initial excitation energy distribution, we took again those data corresponding to the 10 MD runs used for the averaging. The chosen geometry (the exciting laser pulse moves along the $z$-axis and is polarized along the $y$-axis) results in a population somewhat less than 0.8 for chromophore 1 and of less than 0.2 for chromophore 4. The initial populations of chromophore 2 and 3 are more than one order of magnitude smaller. It follows a time trace of the ideal emission spectrum similar to that shown in Fig. 3. A closer inspection indicates, however, that the fluctuations of the spectrum are about five times larger than in the case of a balanced initial chromophore population.

To analyze the emission spectrum in more detail we use the separation, Eq. (23), into partial spectra, Eq. (24), where the single partial emission spectrum $F_{mn}$ is exclusively determined by the single $\sigma_{mn}$. The contributions due to the diagonal density matrix elements are shown in Fig. 4. They nicely display excitation energy redistribution within the first 20 ps to reach a common mean value near 0.25 in the renormalized partial emission spectra. Interestingly, the off-diagonal partial spectra $F_{mn}$ are much smaller (what is not the case for the off-diagonal density matrix elements [11]). This observation also indicates that the approximation Eq. (29) for the spectrum seems to be valid. However, such a behavior is hidden when drawing the total emission rate $F$. The mutual compensation of the structures in the partial spectra has been also observed when choosing other types of initially unbalanced chromophore populations.

We can also state that the fluctuations of the $F_{mm}$ are much smaller than those of the overall spectrum $F$. This is due to the large fluctuations of the off-diagonal partial spectra ($F_{mn}$ with $m \neq n$) around zero. Caused by respective fluctuations of the off-diagonal density matrix elements the resulting fluctuations of $F$ amount 5% of its initial value. Changing to partial spectra following from an initially balanced population of the chromophores the

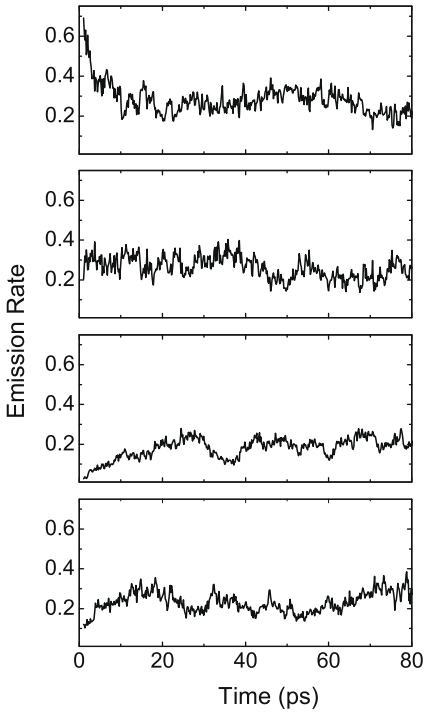


**Fig. 4.** Early part of the $P_4$ time resolved emission (normalized to its initial value and averaged by 10 MD runs as well as by a dephasing time of 20 fs). The initial density matrix is taken as $\sigma_{m,n}(t_0) \sim \delta_{m,n}|\mathbf{d}_m\mathbf{E}|^2$ (the exciting laser pulse moves in $z$-direction with the electric field part $\mathbf{E}$ polarized in $y$-direction, see also text; highest initial population of 0.8 at $m = 1$). Shown are the different (diagonal) partial emission spectra $F_{mm}$, Eq. (24) ($m = 1,\ldots,4$, from top to bottom panel).

fluctuations of the off-diagonal density matrix elements are much smaller (three orders of magnitude compared to those based on an unbalanced initial population).

## 5. Conclusions

The time and frequency resolved emission spectrum of the pheophorbide-*a* complex $P_4$ dissolved in ethanol has been computed in a mixed quantum classical methodology. The quantum part is given by the electronic excitations of the complex while all nuclear coordinates are described classically. This is achieved by carrying out standard room-temperature MD simulations. In order to apply this mixed technique the full quantum formula for the emission spectrum has been translated to the mixed description. Using a particular density matrix theory one may account for radiative decay of the chromophore complex within this mixed description.

A clear indication of excitation energy transfer is obtained if a non-balanced initial distribution is used. It corresponds to an indirect $S_1$-state population of the pheophorbide-*a* molecules via an $S_2$-state optical excitation and a subsequent internal conversion to the $S_1$-state. However, to obtain signatures of excitation energy transfer requires the introduction of partial emission spectra referring to the contribution of a single chromophore. The full emission spectrum only reflects excited-state decay.

## Acknowledgement

Financial support by the Deutschen Forschungsgemeinschaft through Projects RO 1042/17-1 (B.R.) and MA 1356-10/2 (V.M.) are gratefully acknowledged.

## Appendix A. Calculation of the spontaneous emission spectrum

To characterize spontaneous emission we introduce the rate $R_{\lambda\mathbf{k}}(t)$ determining the number of photons emitted per time into the state with polarization $\lambda$ and wave vector $\mathbf{k}$. Since emission appears into the photon vacuum we may set

$$R_{\lambda\mathbf{k}} = \frac{\partial}{\partial t} N_{\lambda\mathbf{k}} = \frac{\partial}{\partial t} \mathrm{tr}\left\{ \widehat{W}(t) a^{+}_{\lambda\mathbf{k}} a_{\lambda\mathbf{k}} \right\}. \tag{A.1}$$

The trace defining the expectation value of the photon-number at time $t$ concerns the CC, the solvent and the photon states. The statistical operator $\widehat{W}(t)$ accounts for the respective time evolution. Consequently, the rate to emit a photon at time $t$ and with energy $\hbar\omega$ reads (note $R_{\lambda\mathbf{k}}(t) \equiv R_{\lambda}(\omega;t)$ and the introduction of a solid angle integration)

$$F(\omega;t) = \frac{V\omega^2}{(2\pi c)^3} \sum_{\lambda} \int do R_{\lambda}(\omega;t). \tag{A.2}$$

It is sufficient for the following to determine the quantity $R_{\lambda\mathbf{k}}$ in second order with respect to the CC–photon interaction $H_{\mathrm{CC-phot}}$, Eq. (13). First, we note

$$R_{\lambda\mathbf{k}} = i\mathrm{tr}\left\{ \hat{h}_{\lambda\mathbf{k}} (a_{\lambda\mathbf{k}} - a^{+}_{\lambda\mathbf{k}}) \widehat{W}(t) \right\}. \tag{A.3}$$

This equation indicates that a restriction becomes possible to an expression for $\widehat{W}$ which is of first-order with respect to $H_{\mathrm{CC-phot}}$. It can be deduced from

$$\widehat{W}(t) = \mathscr{U}_0(t,t_0)\widehat{W}(t_0) - \frac{i}{\hbar}\int_{t_0}^{t} d\bar{t}\, \mathscr{U}_0(t,\bar{t}) \left( \left[ H_{\mathrm{CC-phot}}, \widehat{W}(\bar{t}) \right]_{-} \right), \tag{A.4}$$

which represents the integrated equation of motion for $\widehat{W}$ (the time evolution superoperator $\mathscr{U}_0$ abbreviates the solution of the respective density operator equation at the absence of the CC–photon coupling). Consequently, the second term of the right-hand side is inserted into Eq. (A.3) and the total density operator $\widehat{W}$ is split into a photon part $W_{\mathrm{phot}}$ and a CC-solvent part $\hat{\rho}(t)$. The first has to be chosen as that of the photon vacuum $|\mathrm{vac}\rangle\langle\mathrm{vac}|$ and the latter may be written as

$$\hat{\rho}(t) = \mathrm{tr}_{\mathrm{phot}}\{\widehat{W}(t)\}, \tag{A.5}$$

with the overall density operator $\widehat{W}$ already been introduced in Eq. (A.1).

We further take into account the separation of $\mathscr{U}_0$ into a CC plus (classical) external field part $\mathscr{U}_{\mathrm{CC+field}}$ and a photon part. So, we may finally write:

$$R_{\lambda\mathbf{k}}(t) = 2\mathrm{Re}\int_{t_0}^{t} d\bar{t} e^{-i\omega_{\mathbf{k}}(t-\bar{t})} \mathrm{tr}_{\mathrm{CC+sol}}\left\{ \hat{h}_{\lambda\mathbf{k}} \mathscr{U}_{\mathrm{CC+field}}(t,\bar{t}) \left( \hat{h}_{\lambda\mathbf{k}} \hat{\rho}(\bar{t}) \right) \right\}. \tag{A.6}$$

Note that the trace is reduced to CC and solvent contributions ($\hat{h}_{\lambda\mathbf{k}}$ has been introduced in Eq. (14)). The density operator $\hat{\rho}$ has to be propagated including the exciting external field $\mathbf{E}$. A further propagation of $\hat{h}_{\lambda\mathbf{k}}\hat{\rho}(\bar{t})$ from $\bar{t}$ to $t$ also in the presence of $\mathbf{E}$ is described by the time evolution superoperator $\mathscr{U}_{\mathrm{CC+field}}(t,\bar{t})$.

Now, the CC electronic state part of the trace is taken explicitly (summation with respect to the CC ground-state $\phi_0$ and the singly excited-states $\phi_m$). It remains a trace with respect to all involved vibrational states (of the CC as well as of the surrounding solvent, note the use of Eq. (14))

$$\begin{aligned}
&\mathrm{tr}_{\mathrm{CC+sol}}\left\{ \hat{h}_{\lambda\mathbf{k}} \mathscr{U}_{\mathrm{CC+field}}(t,\bar{t}) \left( \hat{h}_{\lambda\mathbf{k}} \hat{\rho}(\bar{t}) \right) \right\} \\
&= \sum_{m,n} \mathrm{tr}_{\mathrm{vib}}\{ g_{\lambda\mathbf{k}}(m) \langle\phi_0| \left( \mathscr{U}_{\mathrm{CC+field}}(t,\bar{t}) g_{\lambda\mathbf{k}}(n) |\phi_n\rangle\langle\phi_0|\hat{\rho}(\bar{t})\right)|\phi_m\rangle \} \\
&\quad + \sum_{m,n} \mathrm{tr}_{\mathrm{vib}}\{ g_{\lambda\mathbf{k}}(m) \langle\phi_0| \left( \mathscr{U}_{\mathrm{CC+field}}(t,\bar{t}) g^{*}_{\lambda\mathbf{k}}(n) |\phi_0\rangle\langle\phi_n|\hat{\rho}(\bar{t})\right)|\phi_m\rangle \} \\
&\quad + \sum_{m,n} \mathrm{tr}_{\mathrm{vib}}\{ g^{*}_{\lambda\mathbf{k}}(m) \langle\phi_m| \left( \mathscr{U}_{\mathrm{CC+field}}(t,\bar{t}) g_{\lambda\mathbf{k}}(n) |\phi_n\rangle\langle\phi_0|\hat{\rho}(\bar{t})\right)|\phi_0\rangle \} \\
&\quad + \sum_{m,n} \mathrm{tr}_{\mathrm{vib}}\{ g^{*}_{\lambda\mathbf{k}}(m) \langle\phi_m| \left( \mathscr{U}_{\mathrm{CC+field}}(t,\bar{t}) g^{*}_{\lambda\mathbf{k}}(n) |\phi_0\rangle\langle\phi_n|\hat{\rho}(\bar{t})\right)|\phi_0\rangle \}.
\end{aligned} \tag{A.7}$$

The formula can be simplified considerably if some obvious assumptions are taken. First, we account for the fact that the optical preparation of the excited-state is short compared to the emission process and, thus, short compared to the time interval of observation (determined by the time argument $t$). In such a case the time evolution of the emission, given by $\mathscr{U}_{\mathrm{CC+field}}(t,\bar{t})$, can be replaced by a field-free evolution $\mathscr{U}_{\mathrm{CC}}(t-\bar{t})$ (in contrast to the propagation of the density operator which accounts for the external field). We further assume that $\mathscr{U}_{\mathrm{CC}}$ does not cause electronic transitions. Then, due to the orthogonality of the CC electronic states, Eq. (A.7) reduces to the second and the third term on the right-hand side. Since the third term gives an anti-resonant contribution it will be also neglected. Introducing electronic matrix elements of the density operator we get the rate of photon emission

$$\begin{aligned}
R_{\lambda\mathbf{k}}(t) = \frac{4\pi\omega^2_{eg}}{Vh\omega_{\mathbf{k}}} \mathrm{Re}\int_{t_0}^{t} d\bar{t} e^{-i\omega_{\mathbf{k}}(t-\bar{t})} \sum_{m,n,k} \\
\times \mathrm{tr}_{\mathrm{vib}}\left\{ \mathbf{n}_{\lambda\mathbf{k}} \mathbf{d}_m \langle\phi_0| e^{-iH_{\mathrm{CC}}(t-\bar{t})/\hbar} |\phi_0\rangle \mathbf{n}_{\lambda\mathbf{k}} \mathbf{d}^{+}_n \right. \\
\left. \times \hat{\rho}_{nk}(\bar{t}) \langle\phi_k| e^{iH_{\mathrm{CC}}(t-\bar{t})/\hbar} |\phi_m\rangle \right\}.
\end{aligned} \tag{A.8}$$

When calculating the quantity $F(\omega;t)$, Eq. (A.2), we have to carry out a summation with respect to the transversal polarization and a solid angle integration which both result in:

$$\sum_{\lambda}\int do\,[\mathbf{n}_{\lambda\mathbf{k}}\mathbf{d}_m][\mathbf{n}_{\lambda\mathbf{k}}\mathbf{d}_n^+]=\frac{8\pi}{3}\mathbf{d}_m\mathbf{d}_n^+. \tag{A.9}$$

If this expression is used the full quantum rate (rate of ideal time and frequency resolved emission) reads

$$F(\omega;t)=\frac{4\omega^3}{3\pi c^3\hbar}\mathrm{Re}\int_{t_0}^{t}d\bar{t}\,e^{-i\omega(t-\bar{t})}\sum_{m,n,k}\times \mathrm{tr}_{\mathrm{vib}}\Big\{\hat{\rho}_{mn}(\bar{t})\langle\phi_n|e^{iH_{\mathrm{CC}}(t-\bar{t})/\hbar}|\phi_k\rangle e^{-i\mathscr{H}_0(t-t_0)/\hbar}\times[\mathbf{d}_k^{(0)}(t)\mathbf{d}_m^{(0)+}(\bar{t})]e^{i\mathscr{H}_0(\bar{t}-t_0)/\hbar}\Big\}. \tag{A.10}$$

Here, we prevent to take the Condon approximation. The action of the two time evolution operator matrix elements is responsible (after partial Fourier-transformation) for the frequency dispersion of the signal. Note the use of $\langle\phi_0|\exp(-iH_{\mathrm{CC}}(t-\bar{t})/\hbar)|\phi_0\rangle=\exp(-i\mathscr{H}_0(t-\bar{t})/\hbar)$ and of:

$$\mathbf{d}_m e^{-i\mathscr{H}_0(t-\bar{t})/\hbar}\mathbf{d}_n^+=e^{-i\mathscr{H}_0(t-t_0)/\hbar}\mathbf{d}_m^{(0)}(t)\mathbf{d}_n^{(0)+}(\bar{t})e^{+i\mathscr{H}_0(\bar{t}-t_0)/\hbar}, \tag{A.11}$$

with the time-dependent transition dipole matrix elements taken in a representation defined by the CC ground-state vibrational Hamiltonian $\mathscr{H}_0$.

The $\hat{\rho}_{mn}=\langle\phi_m|\hat{\rho}|\phi_n\rangle$ in Eq. (A.10) are defined by the density operator $\hat{\rho}$, Eq. (A.5), reduced to all CC-solvent states (photon contributions have been eliminated). Accordingly, the $\hat{\rho}_{mn}$ remain operators in the vibrational state space and account for excitation energy motion among the different chromophores including respective vibrational dynamics (after optical excitation at $t_0$). For the present application the memory effect ($\bar{t}$ dependence) as well as the account of site off-diagonal elements of the density operator are of some importance. If EET, however, is slow (compared to the decay of the time evolution operator matrix elements), we may replace $\hat{\rho}_{mn}(\bar{t})$ by $\delta_{m,n}P_m(t)\hat{r}_{me}$. This replacement covers the neglect of inter chromophore correlations and characterizes the population of chromophore $m$ (with probability $P_m$) by a vibrational thermal equilibrium distribution (described by the density operator $\hat{r}_{me}$). Moreover, $P_m(t)$ can be removed from the $\bar{t}$ integral with the latter characterizing the line shape of the emission. This corresponds to the standard case where the time-dependence of the emission is determined by the temporal evolution of the excited-state population (see, for example, [22]).

### A.1. Account for CC excitation decay

When entering a nanosecond time region the density matrix is also affected by radiative and non-radiative decay of the CC excitation. An expression has to be introduced from which all degrees of freedom have been removed being responsible for the decay (in the first place the photon states). The reduced density operator introduced in Eq. (A.5) is of such a type being an operator in the complete CC-solvent state space (or later in the electronic CC state space with the nuclear coordinates treated classically).

It is a standard task of dissipative quantum dynamics to derive an equation of motion for the CC density operator $\hat{\rho}$ with a second order account for the CC–photon coupling (see, for example, [22]). Focusing on the excited CC-state contribution, with the dissipative part given in the most simple case (Markov and secular approximation) we arrive at the following equation of motion

$$\frac{\partial}{\partial t}\hat{\rho}_{mn}(t)=-\frac{i}{\hbar}\sum_k(\mathscr{H}_{mk}\hat{\rho}_{kn}(t)-\hat{\rho}_{mk}(t)\mathscr{H}_{kn})-\widehat{D}_{mn}(t,t_0). \tag{A.12}$$

The Hamiltonian matrix has been introduced in Eq. (6) and the dissipative part reads

$$\widehat{D}_{mn}(t,t_0)=\frac{1}{2}(k_m+k_n)\hat{\rho}_{mn}(t). \tag{A.13}$$

This expression comprises population decay in the diagonal part and dephasing of inter-chromophore correlations via the off-diagonal contributions. The $k_m$ include the rates $k_{m\to0}^{(\mathrm{rad})}$ accounting for the radiative excited-state decay of chromophore $m$. They may also cover the rates $k_{m\to0}^{(\mathrm{IC})}$ describing non-radiative decay (internal conversion) as well as the rates $k_m^{(\mathrm{ISC})}$ originated by inter-system crossing to triplet states (ISC rate). Since the $k_m$ do not include the effect of excited-state wave function delocalization (a possible decay out of exciton states [4]) an additional generalization becomes necessary. This all will be the subject of a forthcoming paper [23]. Here, we use a single decay rate $k_m\equiv k$ fitted to experimental data.

## References


[1] M. Fujitsuka, A. Okada, S. Tojo, F. Takei, K. Onitsuka, S. Takahashi, T. Majima, J. Phys. Chem. B 108 (2004) 11935.
[2] E. Hindin, R.A. Forties, R.S. Loewe, A. Ambroise, C. Kirmaier, D.F. Bocian, J.S. Lindsey, D. Holten, R.S. Knox, J. Phys. Chem. B 108 (2004) 12821.
[3] S. Masuo, T. Vosch, M. Cotlet, P. Tinnefeld, S. Habuchi, T.D.M. Bell, I. Osterling, D. Beljonne, B. Champagne, K. Müllen, M. Sauer, J. Hofkens, F.C. De Schryver, J. Phys. Chem. B 108 (2004) 16686.
[4] B. Brüggemann, K. Sznee, V. Novoderezhkin, R. van Grondelle, V. May, J. Phys. Chem. B 108 (2004) 13536.
[5] S. Hackbarth, E.A. Ermilov, B. Röder, Opt. Comm. 248 (2005) 295.
[6] M. Helmreich, E.A. Ermilov, M. Meyer, N. Jux, A. Hirsch, B. Röder, J. Am. Chem. Soc. 127 (2005) 8376.
[7] C. Flors, I. Osterling, T. Schnitzler, E. Fron, G. Schweitzer, M. Sliwa, A. Herrmann, M. van der Auweraer, F.C. De Schryver, K. Müllen, J. Hofkens, J. Phys. Chem. C 111 (2007) 4861.
[8] Y.-Z. Ma, R.A. Miller, G.R. Flemming, M.B. Francis, J. Phys. Chem. B 112 (2008) 6887.
[9] H. Zhu, V. May, B. Röder, M.E. Madjet, Th. Renger, Chem. Phys. Lett. 444 (2007) 118.
[10] H. Zhu, V. May, B. Röder, Th. Renger, J. Chem. Phys. 128 (2008) 154905.
[11] H. Zhu, V. May, B. Röder, Chem. Phys. 351 (2008) 117.
[12] D. Marx, J. Hutter, in: J. Grotendorst (Ed.), Modern Methods and Algorithms of Quantum Chemistry, J. von Neumann Institute for Computing, Jülich, 2000.
[13] S.A. Egorov, E. Rabani, B.J. Berne, J. Chem. Phys. 108 (1997) 1407.
[14] Q. Shi, E. Geva, J. Chem. Phys. 122 (2005) 064506.
[15] M.F. Gelin, D. Egorova, W. Domcke, Chem. Phys. 301 (2004) 129.
[16] T. Meier, Y. Zhao, V. Chernyak, S. Mukamel, J. Chem. Phys. 107 (1997) 3876.
[17] Y. Zhao, T. Meier, W.M. Zhang, V. Chernyak, S. Mukamel, J. Phys. Chem. A 103 (1999) 3954.
[18] V. Chernyak, T. Meier, E. Tsiper, S. Mukamel, J. Phys. Chem. A 103 (1999) 10294.
[19] M.E. Madjet, A. Abdrahman, Th. Renger, J. Phys. Chem. B 110 (2006) 17268.
[20] Z.-W. Qu, H. Zhu, V. May, R. Schinke, J. Phys. Chem. A (2009).
[21] S. Mukamel, Principles of Nonlinear Optical Spectroscopy, Oxford University Press, 1995.
[22] [22] V. May, O. Kühn, Charge and Energy Transfer Dynamics in Molecular Systems, second ed., 2004., Wiley-VCH, Berlin, 2000.
[23] J. Megow, H. Zhu, B. Röder, V. May, in preparation.
[24] O.V. Prezhdo, P.J. Rossky, J. Chem. Phys. 107 (1997) 5863.
[25] J.C. Phillips, R. Braun, W. Wang, J. Gumbart, E. Tajkhorshid, E. Villa, C. Chipot, R.D. Skeel, L. Kale, K. Schulten, Scalable molecular dynamics with NAMD, J. Comput. Chem. 26 (2005) 1781.
[26] W.D. Cornell, P. Cieplak, C.I. Bayly, I.R. Gould, K.M. Merz Jr., D.M. Ferguson, D.C. Spellmeyer, T. Fox, J.W. Caldwell, P.A. Kollman, J. Am. Chem. Soc. 117 (1995) 5179.
[27] J. Wang, R.M. Wolf, J.W. Caldwell, P.A. Kollman, J. Comput. Chem. 25 (2004) 1157.